Geometry-Aligned and Anomaly-Aware Reconstruction for 3D Anomaly Detection

Linchun Wu[1] Qin Zou[1,*] Yuanhan Yue[2] Zhongyuan Wang[1]
[1]Wuhan University, China [2]East China Jiaotong University, China
{linchun.wu, qzou, wzy}@whu.edu.cn, yhyue@ecjtu.edu.cn

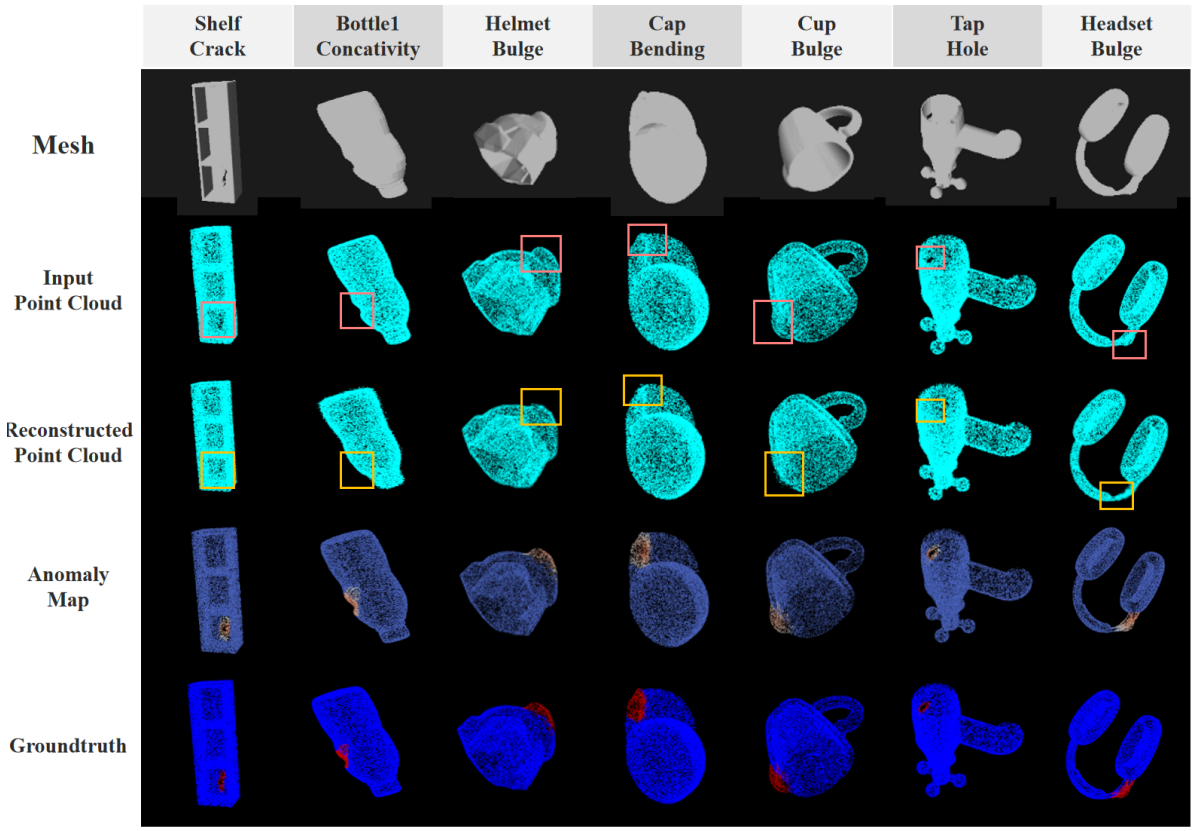

Figure 1. Further reconstruction and detection results of the proposed method on Anomaly-ShapeNet Datasets.

Appendix

Anomaly Synthesis. For anomaly generation, we leverage the off-shelf algorithm DA-Gen from MC4AD as an auxiliary augmentation module. DA-Gen simulates directional defective forces $\mathbf{F}_D$ by perturbing surface normals with controlled randomness to mimic realistic pseudo-anomalies such as scratches and surface distortions. Formally, for each local patch $\hat{\mathbf{P}}_i$, the deformation field is defined as:

$$\mathbf{F}_{D,i} = \left[\beta_i \cdot \lambda_i \cdot \boldsymbol{\nu}_i + (1-\lambda_i) \cdot \boldsymbol{\eta}_i\right] \cdot \gamma_i \cdot \frac{\pi_i}{\max(\pi_i)} \cdot (1 - \sigma_i |\pi_i|), \quad (1)$$

where $\boldsymbol{\nu}_i$ is the surface normal of the i-th patch, $\boldsymbol{\eta}_i$ a randomized direction, and $\beta_i \in \{-1, 1\}$ controls the displacement polarity. λ_i, γ_i, and σ_i regulate the contribution of normal perturbation, displacement magnitude, and defect elongation, respectively. This formulation allows DA-Gen to generate diverse, geometry-consistent anomalies that enhance the robustness of 3D anomaly detection.

Further Visual Proof. We included an extra visual demonstration of our reconstruction and detection results on Anomaly-ShapeNet datasets, please see Figure 1.

P-AUROC on Anomaly Shapenet Dataset. We further provide an extra table of our detection results P-AUROC on Anomaly

Table 1. P-AUROC performance of different methods on Anomaly-ShapeNet across 40 categories, where best and second-place results are highlighted in **red** and **blue**, respectively.

P-AUROC														
Method	**ashtray0**	**bag0**	**bottle0**	**bottle1**	**bottle3**	**bowl0**	**bowl1**	**bowl2**	**bowl3**	**bowl4**	**bowl5**	**bucket0**	**bucket1**	**cap0**
BTF(Raw)(CVPR23')	0.512	0.430	0.551	0.491	0.720	0.524	0.464	0.426	0.685	0.563	0.517	0.617	0.686	0.524
BTF(FPFH)(CVPR23')	0.624	0.746	0.641	0.549	0.622	0.710	0.768	0.518	0.590	0.679	0.699	0.401	0.633	0.730
M3DM(CVPR23')	0.577	0.637	0.663	0.637	0.532	0.658	0.663	0.694	0.657	0.624	0.489	0.698	0.699	0.531
PatchCore(FPFH)(CVPR22')	0.597	0.574	0.654	0.687	0.512	0.524	0.531	0.625	0.327	0.720	0.358	0.459	0.571	0.472
PatchCore(PointMAE)(CVPR22')	0.495	0.674	0.553	0.606	0.653	0.527	0.524	0.515	0.581	0.501	0.562	0.586	0.574	0.544
CPMF(PR24')	0.615	0.655	0.521	0.571	0.435	0.745	0.488	0.635	0.641	0.683	0.684	0.486	0.601	0.601
Reg3D-AD(NeurIPS23')	0.698	0.715	0.886	0.696	0.525	0.775	0.615	0.593	0.654	0.800	0.691	0.619	0.752	0.632
IMRNet(CVPR24')	0.671	0.668	0.556	0.702	0.641	0.781	0.705	0.684	0.599	0.576	0.715	0.585	0.774	0.715
ISMP(AAAI25')	0.865	0.734	0.722	**0.869**	0.740	0.762	0.702	0.706	0.851	0.753	0.733	0.545	0.683	0.672
PO3AD (CVPR'25)	**0.962**	**0.949**	0.912	0.844	0.880	**0.978**	0.914	0.918	0.935	0.967	0.941	0.755	0.899	0.957
MC4AD	0.904	**0.957**	**0.942**	**0.881**	**0.896**	**0.977**	**0.921**	**0.965**	**0.937**	**0.993**	**0.952**	**0.792**	**0.925**	**0.959**
Ours	**0.971**	0.931	**0.955**	**0.927**	**0.934**	0.973	**0.982**	**0.966**	**0.958**	**0.981**	**0.977**	**0.882**	**0.951**	**0.960**

Method	**cap3**	**cap4**	**cap5**	**cup0**	**cup1**	**eraser0**	**headset0**	**headset1**	**helmet0**	**helmet1**	**helmet2**	**helmet3**	**jar0**	**micro.0**
BTF(Raw)(CVPR23')	0.687	0.469	0.373	0.632	0.561	0.637	0.578	0.475	0.504	0.449	0.605	0.700	0.423	0.583
BTF(FPFH)(CVPR23')	0.658	0.524	0.586	0.790	0.619	0.719	0.620	0.591	0.575	0.749	0.643	0.724	0.427	0.675
M3DM(CVPR23')	0.605	0.718	0.655	0.715	0.556	0.710	0.581	0.585	0.599	0.427	0.623	0.655	0.541	0.358
PatchCore(FPFH)(CVPR22')	0.653	0.595	0.795	0.655	0.596	0.810	0.583	0.464	0.548	0.489	0.455	0.737	0.478	0.488
PatchCore(PointMAE)(CVPR22')	0.488	0.725	0.545	0.510	0.856	0.378	0.575	0.423	0.580	0.562	0.651	0.615	0.487	**0.886**
CPMF(PR24')	0.551	0.553	0.551	0.497	0.509	0.689	0.699	0.458	0.555	0.542	0.515	0.520	0.611	0.545
Reg3D-AD(NeurIPS23')	0.718	**0.815**	0.467	0.685	0.698	0.755	0.580	0.626	0.600	0.624	0.825	0.620	0.599	0.599
IMRNet(CVPR24')	0.706	0.753	0.742	0.643	0.688	0.548	0.705	0.476	0.598	0.604	0.644	0.663	0.765	0.742
ISMP(AAAI25')	0.775	0.661	0.770	0.552	0.851	0.524	0.472	0.843	0.615	0.603	0.568	0.522	0.661	0.600
PO3AD (CVPR25')	**0.948**	**0.940**	0.864	0.909	**0.932**	**0.974**	**0.823**	0.907	**0.878**	**0.948**	**0.932**	0.846	0.871	0.810
MC4AD	0.946	**0.940**	**0.925**	**0.917**	0.920	0.951	0.780	**0.932**	**0.885**	**0.926**	**0.874**	**0.879**	**0.877**	0.833
Ours	**0.962**	**0.968**	**0.949**	**0.945**	**0.957**	**0.970**	**0.866**	**0.967**	0.862	0.907	0.861	**0.892**	**0.905**	**0.864**

Method	**shelf0**	**tap0**	**tap1**	**vase0**	**vase1**	**vase2**	**vase3**	**vase4**	**vase5**	**vase7**	**vase8**	**vase9**	**Average**	**Mean Rank**
BTF(Raw)(CVPR23')	0.464	0.527	0.564	0.618	0.549	0.403	0.602	0.613	0.585	0.578	0.550	0.564	0.550	8.675
BTF(FPFH)(CVPR23')	0.619	0.568	0.596	0.642	0.619	0.646	0.699	0.710	0.429	0.540	0.662	0.568	0.628	6.525
M3DM(CVPR23')	0.554	0.654	0.712	0.608	0.602	0.737	0.658	0.655	0.642	0.517	0.551	0.663	0.616	6.850
PatchCore(FPFH)(CVPR22')	0.613	0.733	0.768	0.655	0.453	0.721	0.430	0.505	0.447	0.693	0.575	0.663	0.580	7.800
PatchCore(PointMAE)(CVPR22')	0.543	**0.858**	0.541	0.677	0.551	0.742	0.465	0.523	0.572	0.651	0.364	0.423	0.577	7.950
CPMF(PR24')	0.783	0.458	0.657	0.458	0.486	0.582	0.582	0.514	0.651	0.504	0.529	0.545	0.573	8.450
Reg3D-AD(NeurIPS23')	0.688	0.589	0.741	0.548	0.602	0.405	0.511	0.755	0.624	0.881	0.811	0.694	0.668	5.375
IMRNet(CVPR24')	0.605	0.681	0.699	0.535	0.685	0.614	0.401	0.524	0.682	0.593	0.635	0.691	0.650	5.800
ISMP(AAAI25')	0.701	0.844	0.678	0.687	0.534	0.773	0.622	0.546	0.580	0.747	0.736	0.823	0.691	5.150
PO3AD (CVPR25')	0.663	0.783	0.692	0.955	0.882	0.978	**0.884**	**0.902**	**0.937**	**0.982**	0.950	0.952	0.898	2.735
MC4AD	**0.810**	0.798	**0.777**	**0.969**	**0.889**	**0.990**	0.882	0.875	0.933	**0.995**	**0.953**	**0.959**	**0.910**	**2.125**
Ours	**0.891**	**0.857**	**0.826**	**0.983**	**0.924**	**0.988**	**0.936**	**0.936**	**0.962**	0.985	**0.971**	**0.987**	**0.936**	**1.425**

Shapenet Dataset, our framework averagely outperform the state of the art method by 2% as shown in Table 1.

Normal Reference Impact. For different reference qualities as in Table 2, reconstruction performance degrades with decreasing reference accuracy, while remaining robust within the top-k range.

Table 2. Ablation of different retrieval conditions on Real3D-AD.

Metric	**(Ours)**	Top-k ($k = 5$)	Random	Mismatched
O-AUROC (↑)	**0.820**	0.812	0.726	0.501
P-AUROC (↑)	**0.860**	0.855	0.759	0.477

Chamfer Distance Analysis. To validate the effectiveness of our geometry and vertex rectification modules, we perform Chamfer Distance (CD) evaluation, a widely adopted metric for assessing point distribution similarity in 3D generation tasks. Specifically, we compute the CD between Geometry-Rectified Noisy Points and the input, as well as between Vertex-Rectified Noisy Points and the input, on the Real 3D-AD dataset. As illustrated in Figure 2, geometry rectification achieves an improvement of approximately 0.6 in the CD score, while vertex rectification provides an additional gain of 0.2, clearly demonstrating the effectiveness of the proposed rectification strategy.

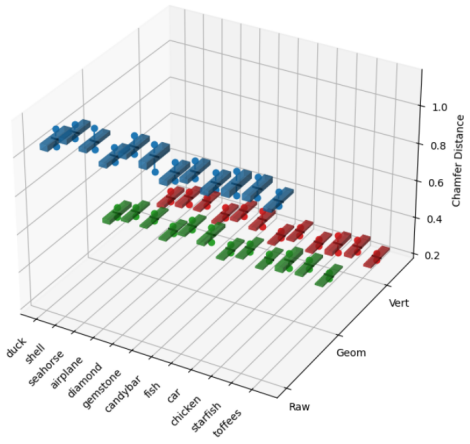

Figure 2. Chamfer Distance Comparison: Noisy-to-Input, Geometry-Rectified Noisy Points-to-Input, and Vertex-Rectified Noisy Points-to-Input on Real 3D AD Datasets. Blue represents standard noise, green denotes Geometry noise and red is Vertex noise.